Vapour-liquid phase transition of dipolar particles

Cite as:
Ganzenmueller, G., Patey, G. N., & Camp, P. J. (2009). Vapour-liquid phase transition of dipolar particles. *Molecular physics*, 107(4-6), 403-413.

Manuscript received: 31/12/2008; Accepted: 07/02/2009; Article published: 20/02/2009

Vapour–liquid phase transition of dipolar particles**

G. Ganzenmüller,[1] G.N. Patey[2] and P.J. Camp[1,*]

[1]EaStCHEM, School of Chemistry, Joseph Black Building, University of Edinburgh, West Mains Road, Edinburgh, EH9 3JJ, UK.

[2]Department of Chemistry, University of British Columbia, 2036 Main Mall, Vancouver, BC, V6T 1Z1, Canada.

[*]Corresponding author; e-mail: philip.camp@ed.ac.uk

[**]G.G. was supported by the UK Engineering and Physical Sciences Research Council (Grant No. EP/D002656/1). The financial support of the Natural Science and Engineering Research Council of Canada is gratefully acknowledged. This work has made use of the resources provided by the Edinburgh Compute and Data Facility (ECDF). The ECDF is partially supported by the eDIKT initiative. The research was also enabled by the use of WestGrid computing resources, which were funded in part by the Canada Foundation for Innovation, Alberta Innovation and Science, BC Advanced Education, and the participating research institutions. WestGrid equipment was provided by IBM, Hewlett Packard, and SGI.

Keywords:
dipolar hard spheres; vapour-liquid transition; Monte Carlo simulation

Abstract

The question of whether a vapour–liquid phase transition exists in systems of particles with purely dipolar interactions is examined. New Monte Carlo simulation results are presented for the dipolar Yukawa hard sphere (DYHS) fluid with very small values of the attractive Yukawa well depth, almost two orders of magnitude smaller than the characteristic dipolar interaction energy. In this way, it is possible to approach the dipolar hard sphere (DHS) limit. It is found that phase separation is not observable beyond a critical value of the Yukawa energy parameter, even though in thermodynamic and structural terms, the DYHS and DHS systems are very similar. It is suggested that either some very subtle physics distinguishes the DYHS and DHS systems, or the observation of a phase transition in DHSs is precluded by finite-size effects.

1. Introduction

Dipolar hard spheres (DHSs) represent the simplest model of polar liquids and colloidal ferrofluids. Despite several decades of intensive theoretical and simulation work, some questions concerning the properties of dipolar fluids remain [1–3]. Many advances in this field have been stimulated by the pioneering and insightful work of Jean-Jacques Weis and his collaborators. The existence of ferroelectric or ferromagnetic fluid phases has been discussed widely [4–9]. Here, we contribute to the long-standing controversy regarding the phase separation of dipolar fluids into coexisting dilute and concentrated isotropic fluid phases. The anisotropic, dipole–dipole (DD) interaction potential reads

$$u_{\mathrm{DD}}(r,\boldsymbol{\mu}_1,\boldsymbol{\mu}_2)=\frac{(\boldsymbol{\mu}_1\cdot\boldsymbol{\mu}_2)}{r^3}-\frac{3(\boldsymbol{\mu}_1\cdot r)(\boldsymbol{\mu}_2\cdot r)}{r^5}, \qquad (1)$$

where $\boldsymbol{r}$ is the centre–centre separation vector, $r=|\boldsymbol{r}|$, and $\boldsymbol{\mu}_i$ is the dipole moment on particle i. The dipolar potential may then be supplemented with either a soft or a hard short-range repulsion to guarantee mechanical stability, and any other relevant interactions for a specific system. DHSs are formed by combination of u_{DD} with the hard sphere (HS) potential

$$u_{\mathrm{HS}}(r)=\begin{cases}\infty, & r<\sigma,\\ 0, & r\geq\sigma,\end{cases} \qquad (2)$$

where σ is the particle diameter. In 1970, de Gennes and Pincus argued that, because the Boltzmann-weighted, angle average of the dipole–dipole potential has a leading order, attractive contribution proportional to $-r^{-6}$, 'on the whole, we expect in 0 field a mechanical phase diagram somewhat similar to that of a conventional Van der Vaals [sic] fluid, with a gas phase, a liquid phase and a solid phase'. Conventional theoretical calculations on DHSs, such as thermodynamic perturbation theory

(e.g. [10]) and integral equations [11] support the existence of a vapour–liquid phase transition. Early simulation results on small systems of DHSs – but without proper treatment of the long-range dipolar interactions – qualitatively confirmed this picture [12]. Direct experimental tests are so far impossible, primarily because of the difficulty in producing monodisperse, single-domain magnetic nanoparticles with sufficiently strong dipole moments.

It came as something of a surprise in the early 1990s when more sophisticated simulation techniques indicated the absence of a vapour–liquid transition in systems of strongly interacting dipolar particles. Gibbs-ensemble Monte Carlo (MC) calculations by van Leeuwen and Smit showed that, when dipolar interactions dominate over short-range isotropic attractions proportional to $-r^{-6}$, a vapour–liquid coexistence region is apparently absent from the phase diagram. Instead, the particles form extended chain-like structures resembling a living-polymer network, stabilised by the energetically favourable nose-to-tail parallel conformation of neighbouring dipoles [13]. The system studied by van Leeuwen and Smit can be mapped on to the Stockmayer (SM) fluid [14], for which the interaction potential is a combination of Lennard-Jones and dipole–dipole terms:

$$u_{\mathrm{SM}}(r, \boldsymbol{\mu}_1, \boldsymbol{\mu}_2) = 4\varepsilon\left[\left(\frac{\sigma}{r}\right)^{12} - \left(\frac{\sigma}{r}\right)^{6}\right] + u_{\mathrm{DD}}(r, \boldsymbol{\mu}_1, \boldsymbol{\mu}_2). \qquad (3)$$

It was observed that the transition disappeared when the characteristic dipolar interaction energy μ^2/σ^3 (with $\mu = |\boldsymbol{\mu}|$) measured against the Lennard-Jones well depth ϵ, exceeded a critical value $\mu^2/\epsilon\sigma^3 = 24.3$ [13–15].

In the case of DHSs, Caillol did not see any sign of phase separation in constant-pressure and Gibbs-ensemble MC simulations at reduced temperatures $k_{\mathrm{B}} T\sigma^3/\mu^2 = 0.18$ and 0.222 16. The chain-like clustering in DHS fluids was thoroughly characterised by Weis and Levesque [17,18].

A number of other model dipolar fluids were studied throughout the 1990s, all seemingly sharing the property that phase separation is somehow precluded by the formation of chain-like clusters. McGrother and Jackson studied hard spherocylinders with longitudinal dipoles as a function of the length (L) to breadth (D) ratio L/D 19 and found that phase separation does not occur below a critical value of $L/D > 0$ (the DHS limit being $L/D = 0$). Szalai *et al*. studied a so-called dipolar Yukawa hard sphere (DYHS) fluid [20] with an interaction potential given by

$$u_{\mathrm{DYHS}}(r, \boldsymbol{\mu}_1, \boldsymbol{\mu}_2) = u_{\mathrm{HS}}(r) + u_{\mathrm{DD}}(r, \boldsymbol{\mu}_1, \boldsymbol{\mu}_2) - \varepsilon_{\mathrm{Y}}\left(\frac{\sigma}{r}\right)\exp[-z(r-\sigma)], \qquad (4)$$

where ϵ_Y is the well depth of the attractive isotropic Yukawa interaction, and $z = 1.8/\sigma$ is a decay parameter. Using the *NPT* + test particle insertion technique, Szalai *et al*. found that condensation exists only for $\mu^2/\epsilon_Y\sigma^3 \leq 9$ [20]. In the light of this collected simulation evidence, several theoretical works set out to explain why the vapour–liquid transition disappears when the propensity for chaining (in the cases above, related to the strength of the dipolar interactions) exceeded some critical level [21–24].

Recent simulation and theoretical results have reignited the controversy. In 2000, Camp *et al*. suggested that, on the basis of MC simulation results, two or more distinct isotropic fluid phases may be present in DHSs [25]. In the same year, Tlusty and Safran presented a mechanism which accommodates phase separation in strongly clustered dipolar fluids [26]; in essence, the transition is driven by the free energies of defects, these being particles at the ends of chains ('end' defects) and particles having three nearest neighbours ('Y' defects). This semi-phenomenological approach has the benefit of acknowledging, at the outset, the presence of very strong positional and orientational correlations between particles, which other theoretical approaches can only hint at through series expansions, integral-equation closures, etc. In 2007, Hentschke *et al*. [27] reported phase separation in the Stockmayer fluid for dipole interaction strengths up to $\mu^2/\epsilon\sigma^3 = 36$, well beyond the limit proposed by van Leeuwen and Smit in 1993 [13]; and Bartke and Hentschke state that a 'van der Waals loop' is visible in the equation of state for a system with $\mu^2/\epsilon\sigma^3 = 100$ [28], which may indicate a phase transition. A critical comparison of all available Stockmayer-fluid results has been presented [29], and an attempt has been made to map the Stockmayer fluid on to DHSs [30]. In 2008, Kalyuzhnyi *et al*.[31] reported phase separation in the DYHS fluid for dipole interaction strengths up to $\mu^2/\epsilon_Y\sigma^3 = 36$, significantly higher than the upper limit proposed by Szalai *et al*. in 1999 [20].

Why are the new results so different from those in earlier works? One possible reason is that many of the pioneering studies employed the Gibbs-ensemble MC technique [32] which is almost certainly going to fail when there is very strong particle association in both the dilute and concentrated coexisting phases [33]; the probability of accepting simultaneous particle deletion in one box and particle insertion in the other is so low that convergence becomes practically impossible. Even single-box simulation techniques, such as constant-pressure MC simulations, have convergence problems due to the low probability of accepting volume changes in low-density systems with almost-percolating networks of particles. In recent times, grand-canonical ensemble simulations have become the method of choice for examining condensation transitions, but these too can run in to problems due to the low probabilities of inserting or deleting particles from extended clusters.

Various strategies have been attempted for sneaking up on purely dipolar systems, starting from models which are relatively easy to simulate. In 2007, Ganzenmüller and Camp studied so-called charged hard dumbbells, charged hard spheres fused in to cation–anion pairs with centre–centre

separation d; DHSs correspond to the limit $d/\sigma \to 0$, and the extrapolation of critical parameters for systems in the range $0.1 \leq d/\sigma \leq 0.25$ yielded estimates for the DHS critical temperature and critical density of $k_B T_c\sigma^3/\mu^2 = 0.153(1)$ and $\rho_c\sigma^3 \simeq 0.1$, respectively [34]. In 2008, Almarza *et al*. [35] studied mixtures of apolar and dipolar hard spheres; extrapolating vapour–liquid critical parameters to the limit of vanishing apolar-sphere concentration yielded estimates for the DHS critical parameters of $k_B T_c\sigma^3/\mu^2 = 0.153(3)$ and $\rho_c\sigma^3 = 0.06(5)$, very close to those obtained by Ganzenmüller and Camp [34].

The existence of a vapour–liquid transition in DHSs has not been confirmed, but the transition in the DYHS fluid for dipolar interaction strengths up to $\mu^2/\epsilon_Y\sigma^3 = 36$ can be clearly seen [31]. In this contribution, the DYHS fluid is revisited in order to see how close one can get to the DHS limit. The data from 31 are supplemented by new MC simulation results for $\mu^2/\epsilon_Y\sigma^3 > 36$, and extrapolations to the DHS limit are attempted. The new results are obtained from grand-canonical Monte Carlo (GCMC) simulations. The problems of sampling and convergence are tackled by employing biased particle insertions and deletions, with some filtering rules to speed up the identification of unfavourable moves. As well as coexistence data being presented, some comparisons are made between the DHS and DYHS fluids in terms of thermodynamic functions and structural properties. This article is organised as follows. In Section 2 the simulation methods are presented. The results are presented in Section 3, and Section 4 contains a critical discussion of the results obtained so far, and an outlook on the problem of dipolar condensation.

2. Simulation methods

The DYHS potential is given in equation (4). Reduced units are defined in the conventional way: reduced temperature $T^* = k_B T\sigma^3/\mu^2$; reduced Yukawa energy parameter $\varepsilon_Y^* = \varepsilon_Y\sigma^3/\mu^2$; reduced dipolar interaction parameter $(\mu^*)^2 = \mu^2/\varepsilon_Y\sigma^3 = 1/\varepsilon_Y^*$; reduced number density $\rho^* = \rho\sigma^3$. With such a definition for ε_Y^*, the DHS limit corresponds to $\varepsilon_Y^* = 0$.

GCMC simulations of the DYHS fluid were performed in a cubic box of volume $V = L^3$, with periodic boundary conditions applied [36,37]. The box lengths spanned the range $10 \leq L/\sigma \leq 22.5$, depending on the other system parameters. The long-range dipolar interaction was handled using the Ewald summation method with conducting boundary conditions; the screening parameter was taken to be $\alpha L = 6$, and the reciprocal space vectors were restricted to the domain $|\boldsymbol{k}| \leq 6 \times 2\pi/L$. The calculation of real-space interactions used lookup tables with Newton–Gregory forward interpolation, and the trigonometric functions that appear in the reciprocal-space Ewald sum were efficiently vectorised using Intel's optimised Math Kernel Library. For the Yukawa potential, a long-range correction was applied in the normal way by assuming that $g(r) = 1$ for $r > L/2$.

Simulations in the grand-canonical ensemble rely on particle insertions and deletions, and so sampling becomes very difficult at low temperatures near T_c where practically all particles are part of a stiff polymer network. The orientation of each dipole is strongly influenced by the local electric field, which is dominated by contributions from its near neighbours. Any unbiased insertion algorithm that generates trial positions and orientations at random will therefore be highly ineffective because the probability of appending a new particle to an existing chain in just the right position and orientation is low. Similarly, random deletion moves will fail in most cases because the majority of particles are part of linear chains and huge energetic penalties are associated with breaking these favourable conformations. An effective insertion/deletion algorithm must therefore meet the following requirements: for insertions, dipole orientations must be chosen in accordance with the local electric field and particles should preferably be appended to existing chains; deletions should preferably remove particles from the ends of existing chains.

Caillol has given a solution to the orientational problem 16 which we have adapted for the grand-canonical ensemble. The local electric field ***E*** is computed at a trial insertion position. Ideally, the orientation of the dipole is drawn from the appropriate Boltzmann distribution of its interaction energy with the field:

$$f(\cos\theta) = \frac{\beta\mu E \exp(\beta\mu E \cos\theta)}{2\sinh(\beta\mu E)}. \qquad (5)$$

A biased trial orientation subtending an angle θ with ***E*** is therefore obtained from

$$\cos\theta = \frac{1}{\beta\mu E}\ln[2R\sinh(\beta\mu E) + \exp(-\beta\mu E)], \qquad (6)$$

where R is a random number generated uniformly on [0, 1].

No highly effective biasing scheme is available to solve the problem of appending and deleting particles from existing chains. Nonetheless, Swendsen–Wang (SW) filter rules can be employed to increase the simulation convergence rate by a large factor [38–40]. The idea of SW filtering is that trial configurations are evaluated using an approximate pair potential which is cheaper to calculate than the full potential. If a trial configuration is energetically unfavourable, then it can be rejected at a reduced computational cost. Of course, this scheme can only work well if a quick and sufficiently accurate predictor is available. In the present case, the predictor was based on an approximate local electric field. Particles were assigned to cells of length 1.25σ, and the electric field was estimated by summing contributions from particles within a central cell and its 26 immediate neighbouring cells. If the approximate energy change accompanying an insertion or deletion was less than 75% of the average insertion or deletion energy for *accepted* moves, then the trial move was rejected with a probability p

$_{SW}$ = 0.9. Additionally, insertions were performed with a higher probability (p_{ins}) than deletions which also improves convergence [41].

The Metropolis acceptance probabilities for insertion ($N \rightarrow N+1$) and deletion ($N \rightarrow N-1$) – taking in to account the SW filter, orientational biasing, and increased insertion probability – are given by

$$p_{N\rightarrow N+1} = \min\left[1, \Theta(p_{SW})\frac{1-p_{ins}}{p_{ins}}\frac{1/2}{f(\cos\theta)}\frac{zV\exp(-\beta\Delta U)}{N+1}\right], \quad (7)$$

$$p_{N\rightarrow N-1} = \min\left[1, \Theta(p_{SW})\frac{p_{ins}}{1-p_{ins}}\frac{f(\cos\theta)}{1/2}\frac{N\exp(-\beta\Delta U)}{zV}\right], \quad (8)$$

where $\Theta(p_{SW})$ is zero with probability p_{SW} if the SW filter condition is not met, and unity otherwise. The factor of $\frac{1}{2}$ accounts for the orientational distribution function $f(\cos\theta) = \frac{1}{2}$ in the ideal-gas reservoir with activity z. As usual, $\beta = 1/k_B T$ and ΔU is the change in configurational energy accompanying the trial move.

It was confirmed that the above sampling scheme is correct by comparing results with those from conventional GCMC simulations. Simulation convergence was monitored by calculating the density–density autocorrelation function $C(\tau) = \langle \delta\rho(\tau)\delta\rho(0) \rangle$, where $\delta\rho(\tau) = \rho(\tau) - \langle \rho \rangle$ and τ is the simulation CPU time. The decay times for $C(\tau)$ with the sampling scheme outlined here are roughly one order of magnitude smaller than those from conventional GCMC simulations.

3. Results

3.1. Critical points

Vapour–liquid coexistence curves for the DYHS fluid with $\varepsilon_Y^* = 0.25$, 0.1111, 0.0625, 0.04, and 0.0278 were presented in 31. In that study, the critical parameters were determined by fitting a standard scaling relation for the near-critical coexistence densities; for completeness, the data are given in Table 1.

ε_Y^*	T_c^*	$(\mu^*)^2$	$k_B T_c/\epsilon_Y$	ρ_c^*	L/σ
0.0125	0.16660(27)	80	13.328(22)	0.0907	15, 17.5, 20, 22.5
0.01875	0.186493(49)	53.3333	9.9463(26)	0.1021	15, 17.5, 20, 22.5
0.025	0.19966(12)	40	7.9862(50)	0.1143	15, 17.5, 20, 22.5
0.0278	0.2061(46)	36	7.42(17)	0.1201(39)	10 (reference 31)
0.04	0.222423(95)	25	5.5606(24)	0.1392	15, 17.5, 20
0.04	0.2227(23)	25	5.567(58)	0.1465(33)	10 (reference 31)
0.0625	0.251456(65)	16	4.0233(10)	0.1687	10, 15, 17.5
0.0625	0.25255((65)	16	4.041(10)	0.1730(23)	10 (reference 31)
0.11111	0.30802(13)	9	2.7722(12)	0.2149	10, 15, 17.5
0.11111	0.30921(66)	9	2.7829(59)	0.2143(15)	10 (reference 31)
0.25	0.46203(41)	4	1.8481(16)	0.2665	10, 15, 17.5
0.25	0.46190(54)	4	1.8476(22)	0.2682(15)	10 (reference 31)
		0	1.2090(18)	0.3184(18)	10 (reference 31)
		0	1.212(2)	0.312(2)	9, 12, 15, 18, 21 (reference 42)

Table 1. Critical parameters for the DYHS fluid. The critical temperatures T_c were determined by finite-size scaling (FSS) fits to results from simulations with the box lengths L indicated; the critical densities ρ_c^* are those from simulations with the largest box lengths. For comparison, data are also shown from 31, which were determined by fitting a universal function to near-critical coexistence data for systems with $L/\sigma = 10$. Note that there are no FSS estimates for the system with $\varepsilon_Y^* = 0.0278$. Results are also shown for the apolar Yukawa hard sphere fluid, corresponding to $(\mu^*)^2 = 0$ [31,42].

This work is focused on determining only the critical parameters, which was achieved using the mixed-field finite-size scaling method introduced by Bruce and Wilding [43]. Briefly, at the apparent finite-size critical point, the probability distribution of the ordering operator $\mathscr{M} = \rho - su$, (where $u = U/V$ is the energy density) falls on to a universal scaling curve, which was assumed to be that of the 3D Ising model $p_{\text{Ising}}(\mathscr{M})$ [44]. (Note that 'dipolar' criticality belongs to a distinct universality class [45] but that the exponents, and presumably the critical ordering-operator distribution, differ only minutely from the Ising results. In any case, the matching of the bimodal distribution serves as a pragmatic means of locating a critical point [46].) GCMC simulations were performed at near-critical conditions where bimodal distributions of the particle number were observed. For each system, up to 100 independent simulations were performed and the joint probability distributions $p(N, U)$ were measured. The results were combined using multiple histogram reweighting [47] in order to find the temperature, chemical potential, and non-universal parameter s that provide the best fit to the universal distribution $p_{\text{Ising}}(\mathscr{M})$. The apparent finite-size critical temperatures $T_c(L)$ then scale like

$$T_c(L) - T_c \propto L^{-(\theta+1)/\nu}, \qquad (9)$$

where θ = 0.54 and ν = 0.6294 are the correction-to-scaling and correlation-length exponents, respectively, for the (assumed) 3D Ising universality class. Examples of MFFSS plots are shown in Figure 1 for systems with $\varepsilon_{\mathrm{Y}}^{*} = 0.0125$, 0.01875, and 0.025; in each case, the system sizes considered were L/σ = 15, 17.5, 20, and 22.5. The uncertainties in T_{c}^{*} quoted in Table 1 are associated with the fitting procedure, and not with systematic errors from any other source. The critical densities showed almost no meaningful finite-size dependence, and so the values reported in Table 1 are simply those for the largest systems simulated. Note that it was possible to observe a vapour–liquid critical point for dipolar interaction strengths almost two orders of magnitude greater than the Yukawa energy.

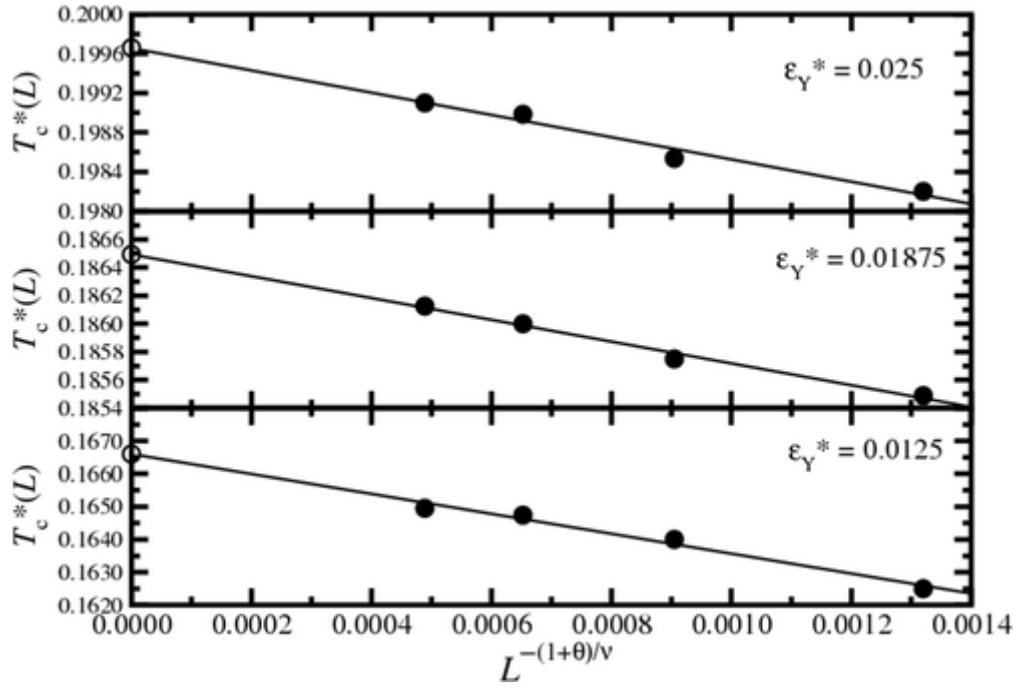

Figure 1. MFFSS plots for the apparent finite-size critical temperature plotted against $L^{-(1+\theta)/\nu}$ for systems with $\varepsilon_{\mathrm{Y}}^{*} = 0.0125$, 0.01875, and 0.025. The points are from simulations, and the lines are fits from Equation (9).

Figure 2(a) shows the reciprocal of the critical temperature in Yukawa units ($\epsilon_{\mathrm{Y}}/k_{\mathrm{B}}T_{\mathrm{c}}$) as a function of the dipolar interaction parameter $(\mu^*)^2$. This plot is suggested by earlier work on the Stockmayer fluid, for which a relationship of the form

$$\frac{\varepsilon_{\mathrm{Y}}}{k_{\mathrm{B}}T_{\mathrm{c}}} = \frac{1}{A + B(\mu^*)^2} \qquad (10)$$

has been noted before 14,29. A fit of equation (10) yields the parameters $A = 1.2051(86)$ and $B = 0.1700(27)$. The resulting fit is shown in Figure 2(a). Note that in the limit $\mu^2/\epsilon_Y\sigma^3 \to \infty$, $k_B T_c \approx B\mu^2/\sigma^3$; B therefore provides an estimate of T_c^* for the DHS fluid in good agreement with other estimates 34,35. Nevertheless, Figure 2(a) may be misleading because equation (10) cannot accurately describe the variation of T_c^* at high values of $(\mu^*)^2$. Figure 2(b) shows a plot of the dipolar critical temperatures T_c^* against ε_Y^*. With smaller values of ε_Y^*, T_c^* follows a sub-linear variation. It was found heuristically that the simulation data could be fitted with a simple function of the form

$$T_c^*(\varepsilon_Y^*) = A\varepsilon_Y^* + B + C\arctan\left(D\varepsilon_Y^*\right). \qquad (11)$$

There is no physical justification for this choice of function, but the combination of a simple saturation function and a linear term does fit the simulation data very well: the fit parameters are $A = 1.0894(24)$, $B = -34.12060(24)$, $C = 21.84370(15)$, and $D = 45907(571)$. (Note, though, that the value of A represents the extrapolated value of $k_B T_c/\epsilon_Y$ at $(\mu^*)^2 = 0$, and that it deviates from the actual values of approximately 1.21 given in Table 1.) A naïve extrapolation of the fitted function suggests that the critical temperature reaches zero at $\varepsilon_Y^* \simeq 0.0025$, implying that there is no phase separation in the DHS limit ($\varepsilon_Y^* = 0$). Attempts were made to find the vapour–liquid critical point in a system with $\varepsilon_Y^* = 0.01$, for which equation (11) predicts that $T_c^* \simeq 0.155$; simulations as far down as $T^* = 0.135$ did not show any sign of phase separation.

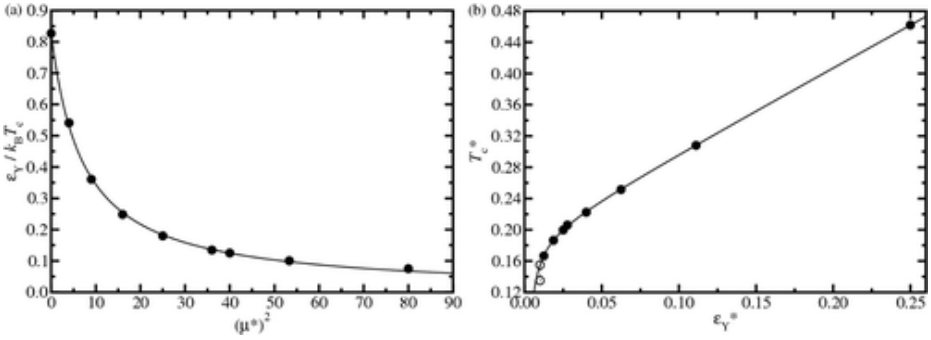

Figure 2. (a) Reciprocal of the critical temperature in Yukawa units $\epsilon_Y/k_B T_c$ versus the dipolar interaction parameter $(\mu^*)^2$. The solid points are the FSS data from Table 1, and the data from 31 for $\mu^2/\epsilon_Y\sigma^3 = 0$ and 36. The solid line is the fit from equation (10). (b) Critical temperature T_c^* against the Yukawa energy parameter ε_Y^*. The solid points are the FSS data from Table 1, and the data from 31 for $\varepsilon_Y^* = 0.0278$. The solid line is the fit from equation (11). The topmost open circle is the extrapolation of the fit to $\varepsilon_Y^* = 0.01$ and $T_c^* = 0.1547$; the open circle below it is the lowest temperature ($T^* = 0.135$) considered in the simulations, and above which no vapour–liquid transition could be found.

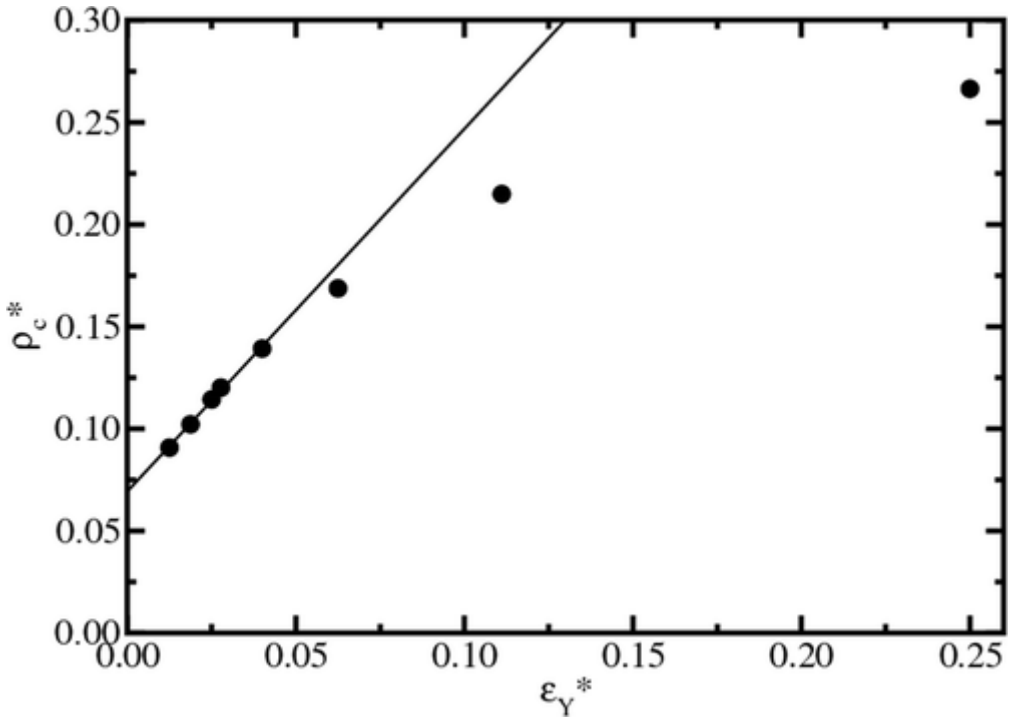

Figure 3. Critical density ρ_c^* against ε_Y^* . The solid points are the FSS data from Table 1, and the data from 31 for $\varepsilon_Y^* = 0.0278$. The solid line is a linear fit to the data for $\varepsilon_Y^* < 0.05$.

The critical density ρ_c^* against ε_Y^* is shown in Figure 3. The data points for $\varepsilon_Y^* < 0.05$ appear to fall on a straight line, and a fit to the equation $\rho_c^*(\varepsilon_Y^*) = A + B\varepsilon_Y^*$ yields the parameters A = 0.0693(16) and B = 1.776(60). A is an estimate of the critical density of DHSs, in good agreement with earlier work [34, 35].

A discussion of the significance of these results is postponed until Section 4, before which results for the thermodynamic and structural properties will be presented.

3.2. Thermodynamics

It is interesting to ask how such small values of the Yukawa energy ϵ_Y, almost two orders of magnitude smaller than the characteristic dipolar energy μ^2/σ^3, have such a strong effect on whether a vapour–liquid transition can be seen in computer simulations. To examine the role of the energy, canonical MC simulations of N = 1024 particles were conducted for the DHS fluid, and for a DYHS fluid with $\varepsilon_Y^* = 0.0125$ (the smallest value for which the transition can still be observed in simulations). For the purposes of comparison, a single isotherm with T^* = 0.15 was considered; this is about 10% below the critical temperature for the DYHS system, and about 2% below the putative

critical temperature for DHSs [34]. The potential energies as functions of the reduced density ρ* are shown in Figure 4. The potential energy for DHSs levels off for densities ρ* ≥ 0.1, but over the range considered, the variations are only on the order of $0.1k_B T$ per particle. For the DYHS system, two sets of data are shown: the total energy – dipolar plus Yukawa – which drops by about $0.3k_B T$ per particle in the range 0.025 ≤ ρ* ≤ 0.3; and the dipolar energy only, which mirrors that of the pure DHS fluid quite closely.

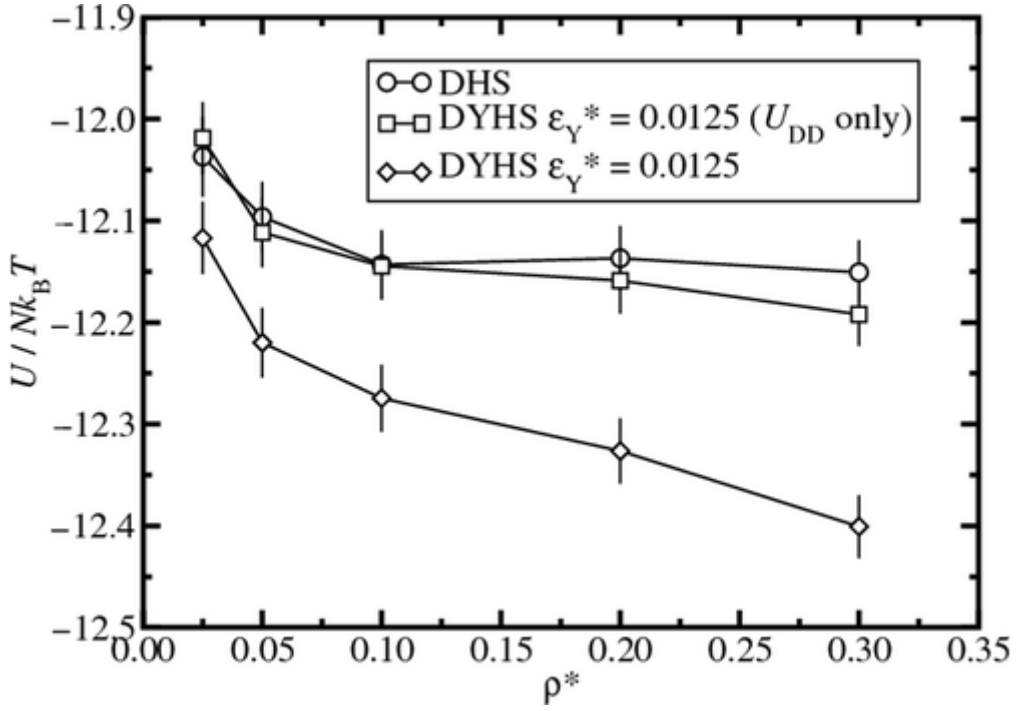

Figure 4. Potential energy per particle in units of $k_B T$ as a function of the reduced density ρ*, at a fixed temperature $T^* = 0.15$. The circles are for pure DHSs. The squares represent the *dipolar energy only* for a DYHS fluid with $\varepsilon_Y^* = 0.0125$ (the lowest value for which phase separation is observable); the diamonds represent the *total energy* (dipolar plus Yukawa) for the same system.

In the classical picture of vapour–liquid phase separation, the vapour phase is of high energy, high enthalpy, and high entropy, while the liquid phase is of low energy, low enthalpy, and low entropy. The temperature-driven transition at fixed pressure is therefore dictated by balances of enthalpy and entropy. The pressure at low temperature is anomalously low (a consequence of strong clustering) and so the addition of the *PV* term to the energy is not going to change the picture very much; a further variation of $0.1–0.2k_B T$ per particle over the density range considered is all that is to be expected 25. It is clear that the classical picture does not apply to DHSs, and it is questionable whether it is relevant

for the DYHS system either. Alternative scenarios include the defect-driven mechanism proposed by Tlusty and Safran [26]. The relevant structural properties of the DHS and DYHS fluids will be discussed next.

3.3. Pair correlation functions

Figure 5 shows the projections of the molecular pair correlation function on to rotational invariants [7,48], determined from canonical MC simulations with $N = 1024$ particles. Two systems are considered, the DHS fluid and the DYHS fluid with $\varepsilon_{\mathrm{Y}}^{*} = 0.0125$, at reduced densities of $\rho^* = 0.025$ and 0.3 and at the same dipolar temperature $T^* = 0.15$ (as inSection 3.2). In order to bring the results for dilute and concentrated phases on to the same scale, the functions $h_{l\,1\,l2\,m}(r)$ are multiplied by ρ^*. Figure 5(a) shows the total pair correlation function $h_{000}(r)$. The essential point is that for a given density, the results for the DHS and DYHS fluids are almost identical, the only noticeable difference being that the peaks are slightly higher and the troughs are slightly shallower in the DYHS fluid than in the DHS fluid; presumably this can be put down to the additional isotropic attraction. For the most part, all of the remaining projections shown in figure 5(b)–(d) exhibit similar features. $h_{112}(r)$ shows a more pronounced deviation between the DHS and DYHS results at high concentration. This projection mirrors the dipolar interaction potential, and the DYHS system seems to possess longer-range correlations of this type. This explains the slightly lower dipolar energy for the DYHS system shown in figure 4. As expected, the functions $h_{110}(r)$ and $h_{220}(r)$ rapidly decay to zero meaning that there is no ferroelectric or nematic ordering at these low densities.

(turn to next page →)

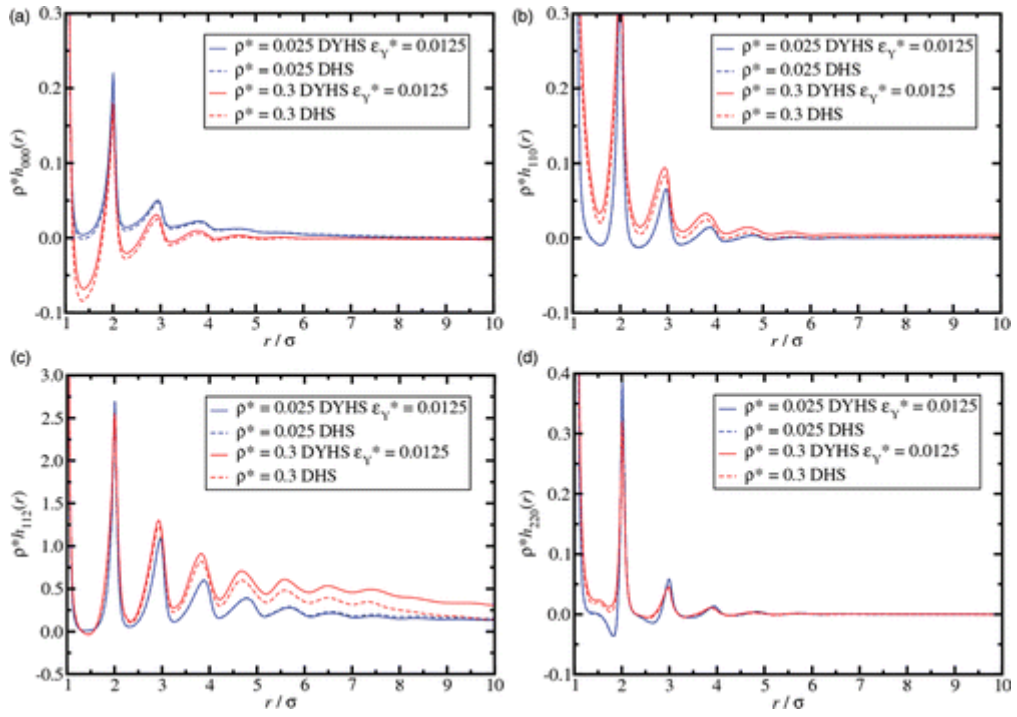

Figure 5. Total correlation functions $h_{l1l2m}(r)$ 7,48 for the DHS fluid and the DYHS fluid with $\varepsilon_{\mathrm{Y}}^{*} = 0.0125$ at a reduced temperature of $T^* = 0.15$ and reduced densities of $\rho^* = 0.025$ and 0.3, representative of the vapour and liquid phases, respectively. The correlation functions are multiplied by the reduced densities in order to bring the results for low and high densities on to the same scale.

3.4. Clustering

The characteristic structural feature of dipolar fluids at low temperatures is the presence of chains and networks. The impact of such clustering on experimentally accessible scattering functions in colloidal ferrofluids is well known [18, 49, 50]. Weis and co-workers have provided in-depth analyses of cluster distributions [17, 51]. Tlusty and Safran have described the structure theoretically in terms of 'end' and 'Y' defects 26. The most simple measure of clustering is the mean cluster size $\bar{n}$. Again, the comparison made here is between the DHS fluid and the DYHS fluid with $\varepsilon_{\mathrm{Y}}^{*} = 0.0125$, at a fixed temperature of $T^* = 0.15$. Table 2 shows results for $\bar{n}$ determined in canonical MC simulations of $N = 1024$ particles at various reduced densities in the range $0.025 \le \rho \le 0.3$. Two particles were considered to be bonded if the dipolar interaction energy between them was less than some cutoff u_c. Using this energy criterion, the system of N particles was partitioned into a set of disjoint clusters, and the mean cluster size $\bar{n}$was computed. The choice of u_c is somewhat arbitrary, so results for several values of u_c in the range $-1.5\mu^2/\sigma^3 \le u_c \le -\mu^2/\sigma^3$ are shown in table 2. The essential point is that, in terms of the mean cluster size, the DHS fluid shows a slightly higher degree of clustering than the DYHS fluid, but only to the extent of a few percent. A reasonable explanation could be that the

isotropic Yukawa interaction increases the possibility of excursions from the ideal nose-to-tail parallel conformation of neighbouring dipoles, resulting in dipolar interaction energies that do not satisfy the clustering criterion. In any case, the deviations are tiny.

		ρ* = 0.025	**ρ* = 0.05**	**ρ* = 0.1**	**ρ* = 0.2**	**ρ* = 0.3**
System	$u_c\sigma^3/\mu^2$	$\bar{n}$	$\bar{n}$	$\bar{n}$	$\bar{n}$	$\bar{n}$
DHS	−1.0	27.20	29.01	29.74	28.89	28.44
DYHS	−1.0	27.02	28.82	29.85	29.53	29.66
DHS	−1.1	19.09	19.20	18.30	15.59	13.40
DYHS	−1.1	18.80	18.73	17.85	15.19	13.29
DHS	−1.2	13.24	13.01	12.17	10.02	8.38
DYHS	−1.2	13.07	12.65	11.73	9.66	8.18
DHS	−1.3	9.06	8.85	8.28	6.88	5.76
DYHS	−1.3	8.97	8.62	7.98	6.62	5.62
DHS	−1.4	6.12	5.99	5.66	4.82	4.12
DYHS	−1.4	6.08	5.86	5.49	4.66	4.03
DHS	−1.5	4.11	4.03	3.85	3.39	2.98
DYHS	−1.5	4.08	3.96	3.76	3.29	2.93

Table 2. Mean cluster sizes $\bar{n}$ for the DHS fluid and the DYHS fluid with $\varepsilon_Y^* = 0.0125$, at a dipolar temperature $T^* = 0.15$ and at various reduced densities ρ*. Results are given for different energy cutoffs u_c.

To shed more light on the cluster structure, coordination-number histograms have been constructed, this time using a distance cutoff criterion of $r_c = 1.1\sigma$. To simplify the analysis, and to make contact with the defect-based theory of Tlusty and Safran [26], each particle has been placed into one of three categories: 'free end', which contains particles with either 0 or 1 nearest neighbour within a distance r_c; 'ideal chain', which contain those particles with 2 nearest neighbours and thus belong to chains; and 'branch', which contain those particles with 3 or more nearest neighbours. Histograms have been computed in canonical MC simulations of the DHS fluid, and DYHS fluids with $\varepsilon_Y^* = 0.0125$ and $\varepsilon_Y^* = 0.025$, at a temperature $T^* = 0.15$ and at densities in the range $0.025 \le \rho^* \le 0.3$; the results are shown in figure 6. In all cases, with increasing density the proportions of particles in the 'free end' and 'ideal chain' categories decrease, while the proportion of 'branch' particles increases. This is broadly in line with the defect-based theory of Tlusty and Safran [26]. At all densities, increasing the Yukawa interaction parameter disfavours 'free ends' and 'ideal chains', but favours 'branches'. This is easily explained by the decreasing net anisotropy of the interactions with increasing ε_Y^*.

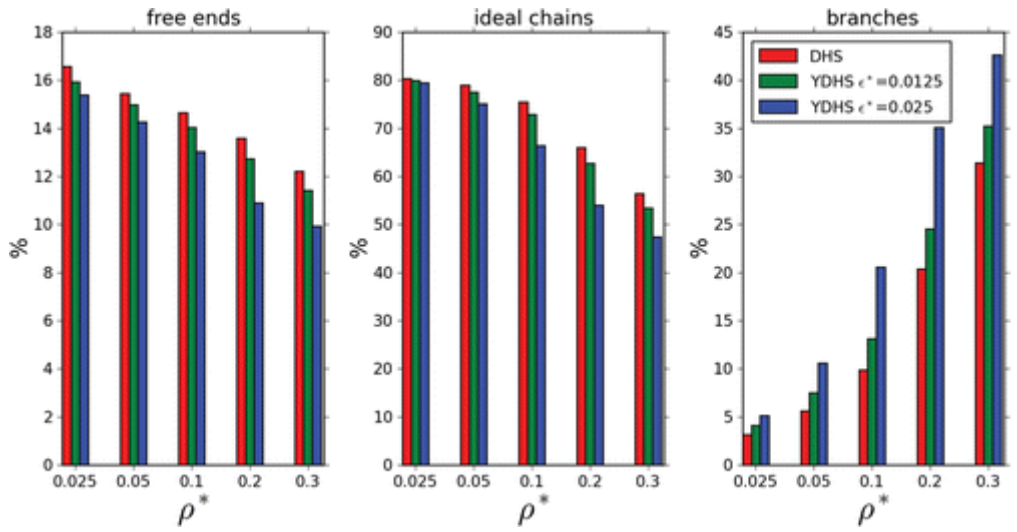

Figure 6. Coordination-number histograms for the DHS fluid (red, left-hand bar), and DYHS fluids with $\varepsilon_{\mathrm{Y}}^{*} = 0.0125$ (green, central bar) and $\varepsilon_{\mathrm{Y}}^{*} = 0.025$ (blue, right-hand bar), at a temperature $T^* = 0.15$ and at densities in the range $0.025 \leq \rho^* \leq 0.3$. The particles are divided into three categories: 'free end', which contains particles with either 0 or 1 nearest neighbour; 'ideal chain', which contain those particles with 2 nearest neighbours and thus belong to chains; and 'branch', which contain those particles with 3 or more nearest neighbours.

4. Summary and discussion

We have presented phase coexistence data from large-scale grand-canonical simulations of dipolar hard spheres (DHSs) interacting with an additional isotropic attractive Yukawa potential, termed dipolar Yukawa hard spheres (DYHSs). In contrast to prior work we have employed a biased particle insertion/deletion Monte Carlo algorithm which has enabled us to study our model in the vicinity of the limit of vanishing isotropic interactions. Critical parameters are presented for systems with Yukawa interaction strengths down to $\varepsilon_{\mathrm{Y}}^{*} = 0.0125$, meaning a well depth almost two orders of magnitude smaller than the characteristic dipolar interaction parameter μ^2/σ^3. Simulations closer to the DHS limit fail to indicate phase separation. Simple extrapolations of the results to the DHS limit yield estimates of the critical parameters in moderate agreement with those from other types of extrapolations. A different extrapolation suited to the low-$\varepsilon_{\mathrm{Y}}^{*}$ regime suggests that the transition disappears before the DHS limit is reached. To gain insight on the differences between the DYHS fluid and the DHS fluid, the configurational energy, pair correlation functions, and cluster statistics have been examined as functions of temperature along a low-temperature isotherm (below the putative critical temperatures). An analysis of the configurational energy shows that even at the highest density considered, the difference between the DYHS and DHS systems is only of order $0.1 k_{\mathrm{B}} T$ per particle. Projections of the molecular pair correlation function on to rotational invariants are

qualitatively similar in the two systems, with only small relative variations in the peaks and troughs. The mean cluster sizes within the two systems differ by only a few percent. The coordination-number histograms for both types of fluid are qualitatively similar, showing decreasing proportions of particles with 0/1 and 2 nearest neighbours as the density is increased, while the proportions of particles with 3 or more nearest neighbours increases. Increasing the Yukawa interaction parameter disfavours particles having 0/1 and 2 neighbours, but favours particles having 3 or more neighbours.

So, the question remains: why, at present, can't the vapour–liquid phase transition be observed in computer simulations of the DHS fluid? Frustratingly, there are no definitive answers to be found in the various quantities measured so far. Therefore, the conclusions are necessarily speculative. With this caveat, two alternative scenarios are proposed which will hopefully help focus future studies.

Scenario 1: *Phase separation does not exist in the DHS fluid.* This is the most obvious conclusion suggested by the simulation results; however, many people have fallen in to this trap before. If this is the correct scenario, then some subtle physics has yet to be uncovered which would explain the apparently different phase behaviour between the DHS and DYHS systems, and the abrupt disappearance of the phase transition when the isotropic interactions are reduced below a critical level. One possible explanation is as follows. In the theory put forward by Tlusty and Safran, vapour–liquid phase separation is considered a demixing transition between 'end' and 'Y' defects, each type of defect making its own contribution to the total free energy of the fluid [26]. Phase separation is predicted for particular ranges of the energetic costs per defect, with the critical temperature and density being dictated only by the values of these energetic parameters. If the theory is correct then the defect energies in the DYHS fluid must be within the necessary ranges for phase separation to occur. Specifically, the energetic cost of an 'end' defect ϵ_1 and the energetic cost of a 'Y' defect ϵ_3 must satisfy the relationship $\epsilon_1 > 3\epsilon_3$; see equation (3) of [26]. It is possible that with the bare dipolar interaction potential, the defect energies are outside of the ranges necessary for phase separation. This would explain the sudden disappearance of the transition as the DHS limit is approached, and is less dramatic than other scenarios such as the existence of a preemptive freezing transition [52], gel formation [53], or a shrinking region of stability of the vapour phase as in some patchy colloids [54].

Scenario 2: *Phase separation cannot be observed in finite-size systems accessible at present.* If phase separation exists in dipolar fluids, and if the mechanism is of the kind proposed by Tlusty and Safran[26], then perhaps the fundamental problem facing simulations is one of finite size. As the isotropic energy parameter in the DYHS system is reduced, the net anisotropy of the interactions increases, leading to a 'stiffer' network and fewer branching points. Perhaps the simulation cell cuts off structures on longer lengthscales, affecting the free energies of the defects, and particularly the 'Y' defects? This kind of effect might perturb the relevant free energies of 'ends' and 'Ys' to a sufficient extent to preclude phase separation. This is not an easy problem to overcome. It is going to be some

time before such accurate calculations can be performed on systems with linear dimensions at least one order of magnitude larger than at present, in order to confirm or deny this scenario. For now, though, it should be made clear that we see absolutely no anomalous system-size effects in the analyses of the critical points.

In our opinion, there is no clear indication at present of how to discriminate between these two scenarios, or alternative scenarios. Despite several decades of theoretical and simulation work, the question of whether a vapour–liquid phase transition exists in systems of particles with purely dipolar interactions still does not seem to have been settled definitively; ongoing work is focusing on other perturbations from the DHS system, including DHSs with truncated interactions, that will at least show which of the phenomena and scenarios described above are universal.

References

[1] Teixeira, PIC, Tavares, JM and Telo da Gama, MM. 2000. *J. Phys.: Condens. Matter*, 12: **R411**.

[2] Huke, B and Lücke, M. 2004. *Rep. Prog. Phys.*, 67: **1731**.

[3] Holm, C and Weis, J-J. 2005. *Curr. Opin. Colloid Interface Sci.*, 10: **133**.

[4] Mamiya, H, Nakatani, I and Furubayashi, T. 2000. *Phys. Rev. Lett.*, 84: **6106**.

[5] Shelton, DP. 2005. *J. Chem. Phys.*, 123: **084502**.

[6] Wei, D and Patey, GN. 1992. *Phys. Rev. Lett.*, 68: **2043**.

[7] Weis, JJ and Levesque, D. 1993. *Phys. Rev. E*, 48: **3728**.

[8] Weis, J-J and Levesque, D. 2005. *Adv. Polym. Sci.*, 185: **163**.

[9] Pounds, MA and Madden, PA. 2007. *J. Chem. Phys.*, 126: **104506**.

[10] Rushbrooke, GS, Stell, G and Høye, JS. 1973. *Mol. Phys.*, 26: **1199**.

[11] Wertheim, MS. 1971. *J. Chem. Phys.*, 55: **4291**.

[12] Ng, KC, Valleau, JP, Torrie, GM and Patey, GN. 1979. *Mol. Phys.*, 38: **781**.

[13] van Leeuwen, ME and Smit, B. 1993. *Phys. Rev. Lett.*, 71: **3991**.

[14] Stevens, MJ and Grest, GS. 1995. *Phys. Rev. E*, 51: **5962**.

[15] Stevens, MJ and Grest, GS. 1994. *Phys. Rev. Lett.*, 72: **3686**.

[16] Caillol, J-M. 1993. *J. Chem. Phys.*, 98: 9835.

[17] Weis, JJ and Levesque, D. 1993. *Phys. Rev. Lett.*, 71: **2729**.

[18] Levesque, D and Weis, JJ. 1994. *Phys. Rev. E*, 49: **5131**.

[19] McGrother, SC and Jackson, G. 1996. *Phys. Rev. Lett.*, 76: **4183**.

[20] Szalai, I, Henderson, D, Boda, D and Chan, K-Y. 1999. *J. Chem. Phys.*, 111: **337**.

[21] Sear, RP. 1996. *Phys. Rev. Lett.*, 76: **2310**.

[22] van Roij, R. 1996. *Phys. Rev. Lett.*, 76: **3348**.

[23] Tavares, JM, Telo da Gama, MM and Osipov, MA. 1997. *Phys. Rev. E*, 56: **R6252**.

[24] Levin, Y. 1999. *Phys. Rev. Lett.*, 83: **1159**.

[25] Camp, PJ, Shelley, JC and Patey, GN. 2000. *Phys. Rev. Lett.*, 84: **115**.

[26] Tlusty, T and Safran, SA. 2000. *Science*, 290: **1328**.

[27] Hentschke, R, Bartke, J and Pesth, F. 2007. *Phys. Rev. E*, 75: **011506**.

[28] Bartke, J and Hentschke, R. 2007. *Phys. Rev. E*, 75: **061503**.

[29] Ganzenmüller, G and Camp, PJ. 2007. *J. Chem. Phys.*, 127: **154504**.

[30] Ivanov, AO, Kantorovich, SS and Camp, PJ. 2008. *Phys. Rev. E*, 77: **013501**.

[31] Kalyuzhnyi, YuV, Protsykevytch, IA, Ganzenmüller, G and Camp, PJ. 2008. *Europhys. Lett.*, 84: **26001**.

[32] Panagiotopoulos, AZ. 1987. *Mol. Phys.*, 61: **813**.

[33] Shelley, JC, Patey, GN, Levesque, D and Weis, JJ. 1999. *Phys. Rev. E*, 59: **3065**.

[34] Ganzenmüller, G and Camp, PJ. 2007. *J. Chem. Phys.*, 126: **191104**.

[35] Almarza, NG, Lomba, E, Martín, C and Gallardo, A. 2008. *J. Chem. Phys.*, 129: **234504**.

[36] Allen, MP and Tildesley, DJ. 1987. *Computer Simulation of Liquids*, Oxford: Clarendon Press.

[37] Frenkel, D and Smit, B. 2001. *Understanding Molecular Simulation: From Algorithms to Applications*, 2, San Diego: Academic Press.

[38] Swendsen, RH and Wang, JS. 1987. *Phys. Rev. Lett.*, 58: **86**.

[39] Frenkel, D. 1992. *Computer Simulation in Chemical Physics, in the NATO ASI Series C*, Edited by: Allen, MP andTildesley, DJ. Vol. 397, 93–152. Dordrecht: Kluwer Academic.

[40] Shelley, JC and Patey, GN. 1995. *J. Chem. Phys.*, 102: **7656**.

[41] Shelley, JC and Patey, GN. 1995. *J. Chem. Phys.*, 103: **8299**.

[42] Pini, D, Stell, G and Wilding, NB. 1998. *Mol. Phys.*, 95: **483**.

[43] Bruce, AD and Wilding, NB. 2003. *Adv. Chem. Phys.*, 127: **1**.

[44] Tsypin, MM and Blöte, HWJ. 2000. *Phys. Rev. E*, 62: **73**.

[45] Aharony, A and Fisher, ME. 1973. *Phys. Rev. B*, 8: **3323**.

[46] Camp, PJ and Patey, GN. 2001. *J. Chem. Phys.*, 114: **399**.

[47] Ferrenberg, AM and Swendsen, RH. 1988. *Phys. Rev. Lett.*, 61: **2635**.

[48] Hansen, J-P and McDonald, IR. 1986. *Theory of Simple Liquids*, London: Academic Press.

[49] Camp, PJ and Patey, GN. 2000. *Phys. Rev. E*, 62: **5403**.

[50] Ivanov, AO, Kantorovich, SS and Pyanzina, ES. 2008. *Magnetohydrodynamics*, 44: **33**.

[51] Tavares, JM, Weis, JJ and Telo da Gama, MM. 1999. *Phys. Rev. E*, 59: **4388**.

[52] Hagen, MHJ and Frenkel, D. 1994. *J. Chem. Phys.*, 101: **4093**.

[53] Blaak, R, Miller, M and Hansen, J-P. 2007. *Europhys. Lett.*, 78: **26002**.

[54] Bianchi, E, Largo, J, Tartaglia, P, Zaccarelli, E and Sciortino, F. 2006. *Phys. Rev. Lett.*, 97: **168301**.